

AIX-MARSEILLE UNIVERSITY

DOCTORAL SCHOOL: Physics and Material Science

PARTENAIRES DE RECHERCHE

Laboratoire MADIREL

Submitted with the view of obtaining the degree of doctor

Discipline: Material Science

Specialty: Characterisation of porous materials

Paul A. Iacomi

Titre de la thèse: sous-titre de la thèse

Defended on JJ/MM/AAAA in front of the following jury:

Prénom NOM	Affiliation	Rapporteur
Prénom NOM	Affiliation	Rapporteur
Prénom NOM	Affiliation	Examineur
Prénom NOM	Affiliation	Examineur
Prénom NOM	Affiliation	Examineur
Prénom NOM	Affiliation	Directeur de thèse

National thesis number: 2017AIXM0001/001ED62



This work falls under the conditions of the Creative Commons Attribution License - No commercial use - No modification 4.0 International.

Abstract

Abstract is here.

Acknowledgements

Acknowledgements go here

Contents

Abstract	iii
Acknowledgements	iv
1. Building a framework for adsorption data processing	1
1.1. Introduction	1
1.2. Physical models of adsorption	2
1.2.1. The Henry model	3
1.2.2. Langmuir and multi-site Langmuir model	3
1.2.3. BET model	5
1.2.4. Toth model	7
1.2.5. Temkin model	7
1.2.6. Jensen-Seaton model	8
1.2.7. Quadratic model	8
1.2.8. Virial model	9
1.2.9. Vacancy solution theory models	9
1.3. Characterisation of materials through adsorption	10
1.3.1. Specific surface area and pore volume calculation	10
1.3.2. Assessing porosity	14
1.3.3. Predicting multicomponent adsorption	19
1.4. pyGAPS overview	21
1.4.1. Core structure	21
1.4.2. Creation of an Isotherm	23
1.4.3. Units	25
1.4.4. Workflow	25
1.4.5. Characterisation using pyGAPS	26
1.5. Processing a large adsorption dataset	33
1.5.1. The NIST ISODB dataset	33
1.5.2. A comparison between surface area calculation methods	35
1.5.3. Variability of the dataset	35
1.6. Conclusion	38
Bibliography	39
2. Extending bulk analysis of porous compounds through calorimetry	44
2.1. Introduction	44
2.2. Energetics of adsorption	45
2.2.1. Forces involved in adsorption	45

2.2.2.	Adsorption thermodynamics	46
2.2.3.	Measuring the enthalpy of adsorption	48
2.3.	Methods	52
2.3.1.	Microcalorimetry	52
2.4.	Results and discussion	52
2.4.1.	Routine characterization of a MOF sample	52
2.4.2.	Analysis of a carbon sample for gas separation applications	53
2.5.	Conclusion	54
	Bibliography	55
3.	Exploring the impact of synthesis and defects on adsorption mea- surements	49
3.1.	Introduction	49
3.2.	The defective nature of MOFs	51
3.2.1.	Types of crystal defects and their analogues in MOFs	51
3.2.2.	Consequences of defects	53
3.2.3.	Defect engineering of MOFs	54
3.2.4.	The propensity of UiO-66(Zr) for defect generation	54
3.3.	Materials and methods	56
3.3.1.	Materials	56
3.3.2.	Methods for quantifying defects	58
3.4.	Results and discussion	59
3.4.1.	Crystallinity of leached samples	59
3.4.2.	NMR	59
3.4.3.	Thermogravimetry results	59
3.4.4.	Nitrogen sorption at 77K	62
3.4.5.	Characterisation of trends	62
3.4.6.	Carbon dioxide isotherms	68
3.5.	Conclusion	69
	Bibliography	70
4.	Exploring the impact of material form on adsorption measurements	78
4.1.	Introduction	78
4.2.	Shaping in context	79
4.3.	Materials, shaping and characterisation methods	81
4.3.1.	Materials	81
4.3.2.	Shaping Procedure	82
4.3.3.	Characterisation of powders and pellets	82
4.3.4.	Sample activation for adsorption	83
4.4.	Results and discussion	83
4.4.1.	Thermal stability	83
4.4.2.	Adsorption isotherms at 77K and room temperature	83
4.4.3.	Room temperature gas adsorption and microcalorimetry	86
4.4.4.	Vapour adsorption	92

4.5. Conclusion	99
Bibliography	100
5. Exploring novel behaviours	104
5.1. Introduction	104
5.2. Literature	104
5.3. Method	104
5.4. Results and discussion	104
5.5. Conclusion	104
Bibliography	105
A. Common characterisation techniques	106
A.1. Thermogravimetry	106
A.2. Bulk density determination	106
A.3. Skeletal density determination	107
A.4. Nitrogen physisorption at 77 K	107
A.5. Vapour physisorption at 298 K	107
A.6. Gravimetric isotherms	108
A.7. High throughput isotherm measurement	108
A.8. Powder X-ray diffraction	108
A.9. Nuclear magnetic resonance	108
Bibliography	108
B. Synthesis method of referenced materials	109
B.1. Takeda 5A reference carbon	109
B.2. MCM-41 controlled pore glass	109
B.3. Zr fumarate MOF	109
B.4. UiO-66(Zr) for defect study	109
B.5. UiO-66(Zr) for shaping study	110
B.6. MIL-100(Fe) for shaping study	110
B.7. MIL-127(Fe) for shaping study	110
Bibliography	111
C. Appendix for chapter 4	112
C.1. Calorimetry dataset UiO-66(Zr)	112
C.2. Calorimetry MIL-100(Fe)	113
C.3. Calorimetry MIL-127(Fe)	116
Bibliography	116

2. Extending bulk analysis of porous compounds through calorimetry

2.1. Introduction

While the previous chapter focused on a physical description of adsorption and its use for the characterisation of porous materials, a rigorous thermodynamic background was omitted. However, an understanding of the energetic aspects of adsorption allows for one of the most powerful applications of adsorption methodology, namely a representation of the kinds of physical and chemical processes occurring during adsorption. Through a direct or indirect measurement of the so-called enthalpy of adsorption (h_{ads}), information about surface composition, the strength of adsorbate-guest and guest-guest interactions, phase change phenomena and, in some cases, transitions in the adsorbing material itself can be obtained.

Furthermore, the enthalpy of adsorption is a crucial parameter in an industrial setting. Owing to the exothermic nature of adsorption in combination with the strong influence of temperature on the performance of adsorbent materials, h_{ads} is often regarded as the most important parameter in the design of beds and columns, alongside working capacity and adsorption/catalytic selectivity. The enthalpy of adsorption is also a measure of the guest-host interactions, which have to be overcome for material regeneration. As such, it represents an important metric of the energy efficiency of the process.

As such the insight afforded through measurement of the energetic components of adsorption can prove invaluable for investigating subtle changes in adsorbent materials which lead to the kind of variability encountered in chapter 1. The thoroughness and suitability of the activation procedure, presence of surface functionalisations, defect formation such as inclusion of counterions and vacancies and activation-driven phenomena such as gate opening, state switching or flexibility all be qualitatively and, with careful methodology, even quantitatively analysed.

Chapter summary

First, an overview of the theoretical aspects underpinning the energetics of adsorption is presented. The methods section will go into detail in the available methodology for studying the enthalpy of adsorption on surfaces and in pores. The final part of the chapter will explore the use of combined adsorption and calorimetric measurements as a way of extending characterisation of porous materials.

Contributions

The sample of Zr Fumarate MOF was synthesised in the group of Prof. Peter Behrens, from the University of Hannover, Germany. All measurements on this sample and data processing were performed by Paul Iacomi in the Madirel Laboratory, Marseille.

2.2. Energetics of adsorption

2.2.1. Forces involved in adsorption

From a classical molecular point of view, we can define the guest-host and guest-guest interactions as a sum of several components with distinct physical meaning.

$$\Phi_t = \Phi_R + \Phi_D + \Phi_C + \Phi_I \quad (2.1)$$

The first two types of interaction, namely short range electrostatic repulsion between the electron clouds of neighbouring atoms Φ_R and long range dispersion Φ_D arising from incidental short-lived partial charges are common to all atoms, and can therefore be called “non-specific”. Such interactions are commonly modelled through the use of a Lennard-Jones type potential function.

$$V_{LJ} = 4\epsilon \left[\left(\frac{\sigma}{r} \right)^{12} - \left(\frac{\sigma}{r} \right)^6 \right] \quad (2.2)$$

The latter two types, Coulombic interactions Φ_C and induction interactions Φ_I arise from permanent charges and multipoles in the system. Coulombic interactions are attraction and repulsion interactions between charges such as molecular ions, permanent dipoles and quadrupoles. Induction, also known as polarization or Debye forces, is the interaction between a charged particle or a multipole with the induced multipole in a non-charged system. The ease of inducing such an interaction in a molecule is termed polarizability. These interactions can be referred to as “specific”.

Therefore, in the standard definition of adsorption, only Van-der-Waals forces are responsible. However, depending on the systems involved, stronger interactions such as hydrogen bonding, electron sharing, stacking or π interactions may also play a role in the overall stability of the guest-host attraction.

The total interactions can also be broken down as contributions from guest-host interactions and guest-guest interactions. If changes in the adsorbent occur as a result of adsorption, a host-host or self-potential interaction should be considered. The guest-host interaction can be assumed constant for a homogeneous surface or a function of coverage, in the case of a heterogeneous surface.

2.2.2. Adsorption thermodynamics

As mentioned in the previous section, adsorption is a consequence of intermolecular attraction between the material surface and the molecules of the fluid. The sum of all interactions accounts for the depth of the potential well and therefore for the energy corresponding to the process. As this energy is net positive, adsorption is an overall exothermic phenomenon.

However, in order to make the transition from a molecular viewpoint to a macroscale bulk fluid representation of adsorption, the a thermodynamic description of the adsorbed phase of the process must be performed.

The Gibbs surface excess approach

A description of the adsorbed phase can be made through expressing the change in density or concentration of fluid from the adsorbent surface to the bulk phase. The density has a maxima in the immediate zone close to the surface, and then decreases until it reaches the density of the bulk fluid. However, when defined as such, the boundary between the two phases is difficult to pinpoint. Therefore, in most cases it is useful to employ the concept of the Gibbs dividing surface.

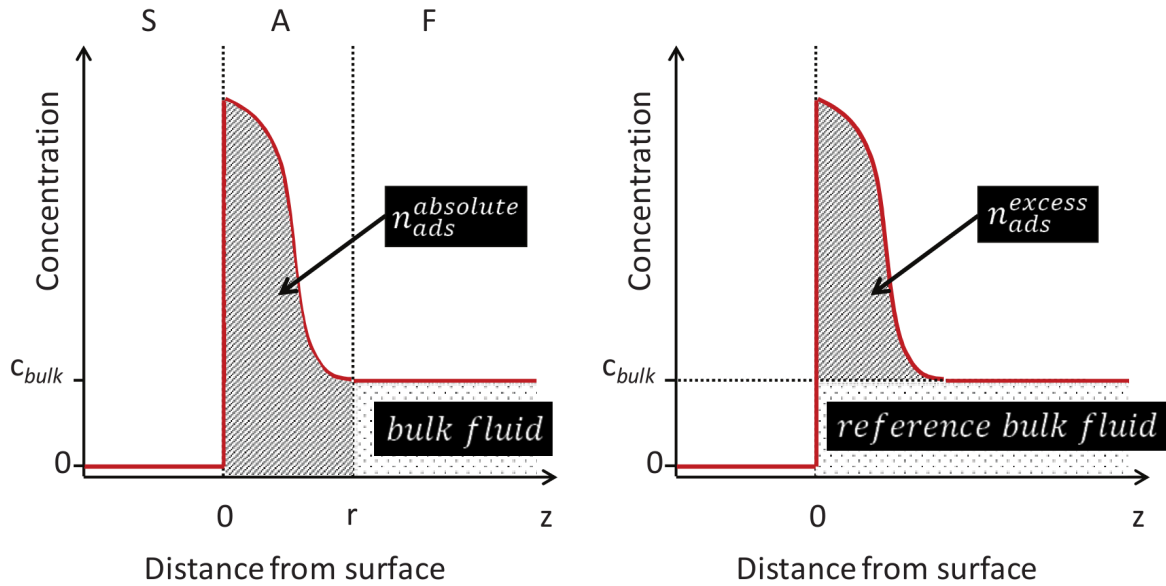


Figure 2.1.: Representation of the adsorbed and bulk phases according to the (left) layer model and the (right) Gibbs dividing surface approach. Adapted from Rouquerol et al..⁽¹⁾

This approach describes the adsorbed phase only in terms of an *excess* from the properties of the bulk phase. As represented in Figure 2.1, the total amount adsorbed

2. Extending bulk analysis of porous compounds through calorimetry

can be defined as:

$$n_{ads}^a = A \int_0^r c \, dz \quad (2.3)$$

The imaginary Gibbs dividing surface is usually placed parallel to the real surface of the adsorbent and in the resulting system, the concentration of the adsorbent in the adsorbed phase are expressed as an excess from the concentration of the bulk fluid. The relationship between the total amount adsorbed and the excess amount adsorbed is then:

$$n_{ads}^\sigma = n_{ads}^a + V_{ads} \cdot c_{bulk} \quad (2.4)$$

As long as the volume of the adsorbed layer V_{ads} can be considered negligible and the concentration of adsorbate in the bulk phase c_{bulk} is low, the total amount adsorbed and the surface excess amount may be considered as approximately equal. This is usually the case for experiments such as nitrogen adsorption at 77 K, or room temperature adsorption below 1 bar. At high pressures or when the difference in concentration between the adsorbed and the bulk phase is low, the total amount adsorbed begins to diverge significantly from the surface excess.

Without corrections, both the gravimetric and manometric method of adsorption will measure excess amounts adsorbed. In the case of adsorption in porous materials, the volume of the adsorbed phase may be taken as total pore volume.

Differential enthalpy of adsorption

Adsorption can be considered as a closed system of constant volume V and temperature T . No mass of material crosses the system boundary, therefore the total change in chemical potential is also zero $d\mu = 0$. Through a derivation⁽¹⁾ of the gas and adsorbed phase/adsorbent energies we may obtain a Gibbs-Duhem type equation:

$$d\mu^\sigma = -\frac{S^\sigma}{n^\sigma}dT + \frac{A}{n^\sigma}d\pi \quad (2.5)$$

from which the Gibbs adsorption isotherm (Equation 1.1) may be derived, as well as

$$\ln p = \frac{\dot{u}_{T,\Gamma}^\sigma - u_T^g - RT}{RT} - \frac{\dot{s}_{T,\Gamma}^\sigma - s_0^g}{R} = \frac{\Delta_{ads}\dot{h}_{T,\Gamma}}{RT} - \frac{\Delta_{ads}\dot{s}_{T,\Gamma}}{R} \quad (2.6)$$

an expression relating the differential enthalpy of adsorption $\Delta_{ads}\dot{h}_{T,\Gamma}$ and the differential entropy of adsorption $\Delta_{ads}\dot{s}_{T,\Gamma}$ to the pressure of an ideal gas. The relationship between the differential enthalpy and the differential energy of the adsorbed phase is given by:

$$\Delta_{ads}\dot{h}_{T,\Gamma} = \Delta_{ads}\dot{u}_{T,\Gamma} - RT \quad (2.7)$$

Application of differential enthalpy of adsorption to the characterisation of materials

As the differential enthalpy of adsorption represents the interactions taking place during adsorption, it is often used in conjunction with the isotherm to study the properties of adsorbent materials. Unfortunately, only the total sum of all interactions is measurable through direct methods. Therefore, the absolute contribution of each component presented in subsection 2.2.1 cannot be determined. However, with careful choice of experiments and interpretation of results, specific components may be compared.

Effect of structure of the guest on guest-host interactions can be investigated for example through changing the Si/Al ratio in a series of MFI zeolites.⁽²⁾ The role of compensation cations in a ion-exchanged X-faujasite⁽³⁾ or the influence of open metal sites⁽⁴⁾ and their distribution⁽⁵⁾ can be assessed through analysis of the calorimetry curves. The contribution of non-specific effects such as π backbonding⁽⁶⁾ can be seen by the choice of a suitable probe pair, such as a saturated and unsaturated version of hydrocarbons (ethane/ethylene/acetylene). Guest-guest interactions during adsorption may also be monitored, such as cooperative effects such as 2-dimensional analogues of phase changes.⁽⁷⁾ If the adsorbate itself undergoes changes during adsorption, as is the case in soft materials, the measured enthalpy of adsorption can be a clear indication of such changes in structure.⁽⁸⁾ The net enthalpy of adsorption in such a system is often lowered through the energetic contribution of the state change of the adsorbate and may be of use for a reduction in the thermal load to be dissipated for adsorption or required to recover the adsorbed material.⁽⁹⁾

The differential enthalpy of adsorption is often represented as a function of partial coverage. In Figure 2.2, isotherm types as defined by IUPAC are presented together with a typical differential enthalpy curve. Type I isotherms often have an initial plateau, corresponding to adsorption in micropores until a sharp decrease at complete pore filling occurs. If the surface of the pores is heterogeneous, higher energy sites will be occupied first, resulting in a sharp slope at low loadings. Multilayer adsorption in non-porous or mesoporous materials (II and IV) yields a slowly decreasing enthalpy curve, as the solid-guest interactions drop off with increasing layers adsorbed. Finally, cooperative adsorption, as seen in a type III isotherm, often gives rise to initial enthalpies of adsorption which are below the enthalpy of vaporisation. It should be noted that changes in the adsorbed fluid similar to phase changes may occur, which can be seen in the enthalpy curve as a distinct peak.^(2,7,10)

2.2.3. Measuring the enthalpy of adsorption

Experimentally, two methods are widely used for determining the enthalpy of adsorption. The first relies on measurement of two or more isotherms at different temperatures and the use of a Clausius-Clapeyron-type equation for indirect calculation, while the second is a direct measurement of the evolved heat during adsorption using calorimetry.

A value for the enthalpy of adsorption in a particular system may also be obtained from computer simulation methods. The accuracy of these procedures depends on the

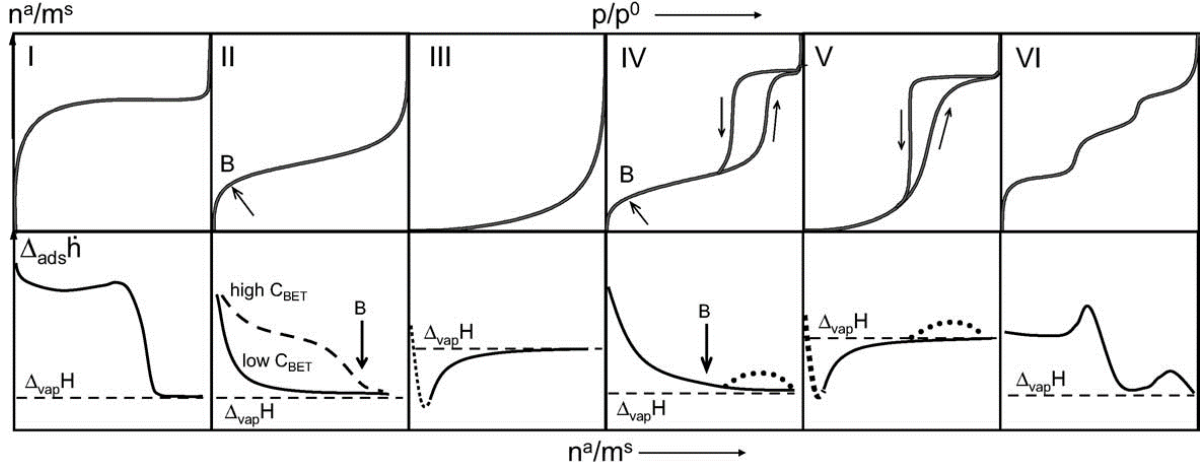


Figure 2.2.: Generalized curves of differential enthalpy of adsorption with respect to coverage corresponding to different IUPAC-defined isotherm types. Adapted from Llewellyn and Maurin.⁽¹¹⁾

accuracy of the chosen model of interaction between simulated molecules.

Isosteric enthalpy of adsorption

If the differential enthalpy of adsorption is assumed be independent of temperature, Equation 2.6 can be differentiated with respect to temperature keeping the surface adsorbed amount constant to obtain an equation analogous to the Clausius-Clapeyron equation:

$$\left(\frac{\partial \ln p}{\partial T}\right)_{n_a} = -\frac{\Delta_{ads}\dot{h}_{T,\Gamma}}{RT^2} \quad (2.8)$$

The equation can be rearranged to calculate the differential enthalpy:

$$\Delta_{ads}\dot{h}_{T,\Gamma} = R\left(\frac{\partial \ln p}{\partial 1/T}\right)_{\Gamma} \quad (2.9)$$

where $\Delta_{ads}\dot{h}_{T,\Gamma}$ is the often termed the isosteric enthalpy of adsorption.

In order to approximate the partial differential, two or more isotherms are measured at different temperatures. Afterwards the isosteric enthalpy of adsorption can be calculated by using the pressures at which the loading is identical using the rearranged equation. By plotting the values of $\ln p$ against $1/T$ we should obtain a straight line with a slope of $-\Delta_{ads}\dot{h}_{T,\Gamma}/R$.

As experimental isotherms do not necessarily have points spaced at equal loading intervals, often interpolation is used to obtain data at the desired points. Alternatively, a model may be used to first fit the isotherm, which is then used for the calculation.

The isosteric enthalpy is sensitive to differences in pressure between the two isotherms. If the isotherms measured are too close together, the error margin will increase. The

2. Extending bulk analysis of porous compounds through calorimetry

method also assumes that isosteric enthalpy does not vary with temperature. If the variation is large for the system in question, the calculation will give unrealistic values.

Even with carefully measured experimental data, there are two assumptions used in deriving Equation 2.9: an ideal bulk gas phase and a negligible adsorbed phase molar volume. These have a significant effect on the calculated isosteric enthalpy of adsorption, especially at high relative pressures and for heavy adsorbates.

Microcalorimetry

A direct measurement of the enthalpy of adsorption is possible using calorimetric methods. An isothermal calorimeter is most often used for this purpose, to best approximate a reversible exchange of heat between the system under investigation and the surrounding heat sink. To allow for a complete integration of evolved heat, with minimal losses, a 3D Tian-Calvet thermopile⁽¹²⁾ can be used. In order to cancel out variations in environment, differential mounting is employed, in which the signal is the difference in voltage between a reference and experimental thermopile. In order to ensure the “isothermicity” of the calorimeter, a suitable heat sink must be used, leading to two types of design. Ambient temperature calorimeters use resistance heating to maintain the internal temperature while utilising the environment as its heat sink. At low temperature, the environment acts as a heat source and therefore the heat sink must be provided, often in the form of a constant-temperature bath undergoing a phase change or through a cryostat. Sketches of an ambient and a low temperature differential Tian-Calvet calorimeter can be seen in Figure 2.3.

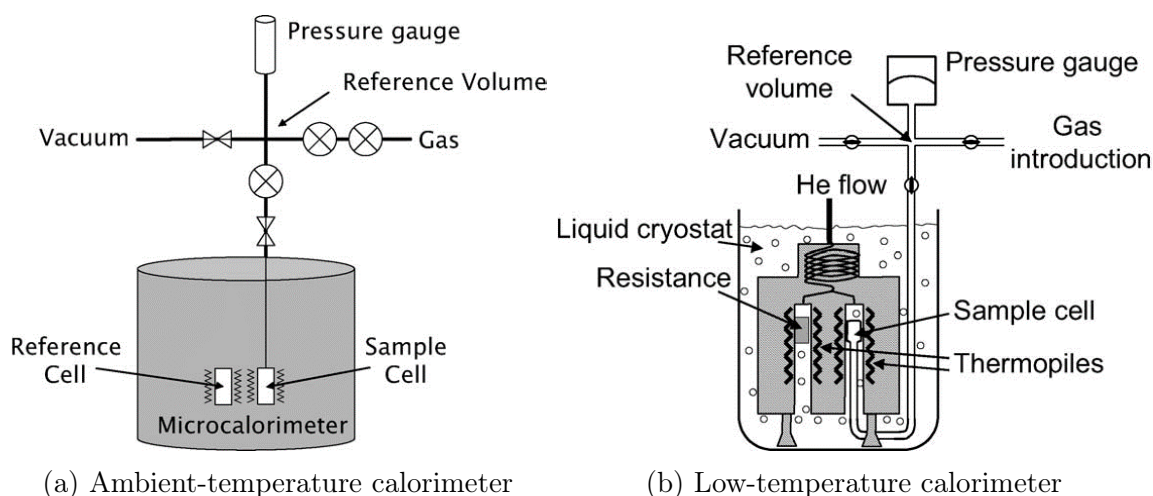


Figure 2.3.: Two types of isothermal Tian-Calvet calorimeters for adsorption measurements, specialized for different temperature ranges. Adapted from Llewellyn and Maurin.⁽¹¹⁾

Care must be taken to ensure that the recorded heat through such an experiment can be related directly to adsorption enthalpy and not to other heat effects. The accepted convention⁽¹³⁾ is that the adsorbate itself is inert and therefore does not contribute to

2. Extending bulk analysis of porous compounds through calorimetry

the variation of any state function. The heat which is measured through calorimetry corresponds to two components, the differential enthalpy of adsorption and the work required to expand the gas into the measurement cell. In this relationship as expressed in Equation 2.10 the value for work can be substituted by $V\Delta P$ and accounted for at each point.

$$\dot{Q} = \Delta_{ads}\dot{h} + W \quad (2.10)$$

$$\dot{Q} = \Delta_{ads}\dot{h} + V\Delta P \quad (2.11)$$

$$\Delta_{ads}\dot{h} = \dot{Q} - V\Delta P \quad (2.12)$$

Finally, to obtain a value for the differential enthalpy of adsorption, the enthalpy is divided by the amount of gas adsorbed in the same time.

Two options exist regarding the method of introduction of adsorbate: the continuous and the discontinuous or point-by-point method. In the point-by-point method, discrete insertion steps made. A reference volume is filled with gas at a pressure p , which is allowed to equilibrate before a valve between the reference volume and the cell containing the adsorbate. In the other method, the flow of adsorbate is continuous, usually kept constant by a restriction in the pipe diameter which is severe enough to allow the gas to enter sonic flow regimes. At this point, the flowrate is no longer influenced by a pressure differential, instead becoming a function only of upstream pressure and environment temperature. The heat evolved during adsorption (or required during desorption) is therefore measured either as discrete peaks, corresponding to each event or as a continuous heat curve. An example of such a signal for each method presented in .

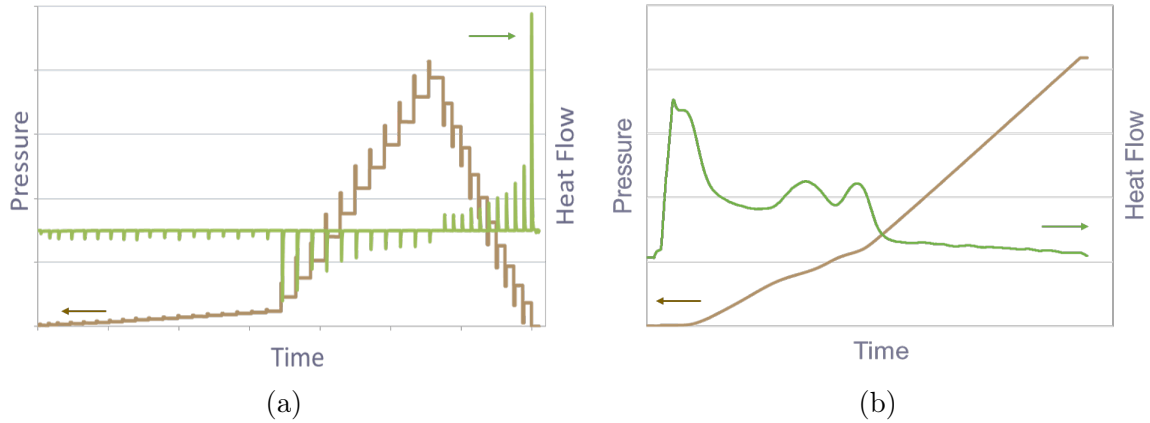


Figure 2.4.: Typical pressure and calorimeter signals for the two available methods of introducing adsorbate into the measurement cell (a) discontinuous and (b) continuous.

The point-by-point method is less accurate than a continuous introduction, as the measured heat is necessarily a cumulative value of instantaneous differential enthalpy

for the coverage range of each adsorbed point. However, it has the advantage of ensuring complete equilibrium at each step, by observing the return to the baseline of the calorimetry signal or a stable pressure signal. On the other hand, the continuous method allows for subtle changes in the differential enthalpy of adsorption, such as those corresponding to adsorbed phase changes, to be seen experimentally. Additionally, the time-resolved data can be used to investigate transient phenomena. Equilibrium between the adsorbed phase and gas phase is no longer guaranteed, and must be tested for by performing multiple experiments at different adsorbate flowrates. Alternatively, the experiment can be stopped to observe that the time for the heat signal to return to its baseline does not diverge from the dead time of the calorimeter.

2.3. Methods

2.3.1. Microcalorimetry

In this thesis, combined isotherms and enthalpy of adsorption measurements were made experimentally using a Tian-Calvet type microcalorimeter coupled with a home-made manometric gas dosing system.⁽¹¹⁾ This apparatus allows the simultaneous measurement of the adsorption isotherm and the corresponding differential enthalpies. Gas is introduced into the system using a step-by-step method and each dose is allowed to stabilize in a reference volume before being brought into contact with the adsorbent located in the microcalorimeter. The introduction of the adsorbate to the sample is accompanied by an exothermic thermal signal, measured by the thermopiles of the microcalorimeter. The peak in the calorimetric signal is integrated over time to give the total energy released during this adsorption step. At low coverage the error in the signal can be estimated to around $\pm 0.2 \text{ kJ mol}^{-1}$. Around 0.4 g of sample is used in each experiment. For each injection of gas, equilibrium was assumed to have been reached after 90 minutes. This was confirmed by the return of the calorimetric signal to its baseline ($< 5 \text{ } \mu\text{W}$).

Data processing

2.4. Results and discussion

2.4.1. Routine characterization of a MOF sample

New materials are often screened for their ability to act as a CO_2 capture material. A good predictor of performance in this application are the enthalpies of adsorption, which are an indication of host-guest interactions. Here, we first measure the differential heats of adsorption directly through the use of adsorption microcalorimetry at 303 K. Then, to determine the isosteric heats of adsorption, two isotherms have been measured at 303 K and 323 K respectively. The complete set of isotherms is loaded into `pyGAPS` and plotted by the `pygaps.plot_iso()` function as seen in Figure ???. To calculate the isosteric heat of adsorption, the two isotherms measured for this purpose are passed through the

2. Extending bulk analysis of porous compounds through calorimetry

`pygaps.isosteric_heat()` function. The results from the calculation are overlaid on top of the measured calorimetric data in Figure ???. The two datasets are overlap for the most part but diverge at low loadings and near complete coverage. At low loading the small changes in pressure amount introduce large errors in the Clausius-Clapeyron equation. This, together with the breakdown of the assumption of equilibrium due to active sites in the MOF lead to the calorimetric measurement providing more valid results. At higher loadings, where the isotherm reaches a plateau and the change in adsorbed amount is small from point to point, errors are introduced in the direct calculation of the heat of adsorption. The two techniques are thus complementary.

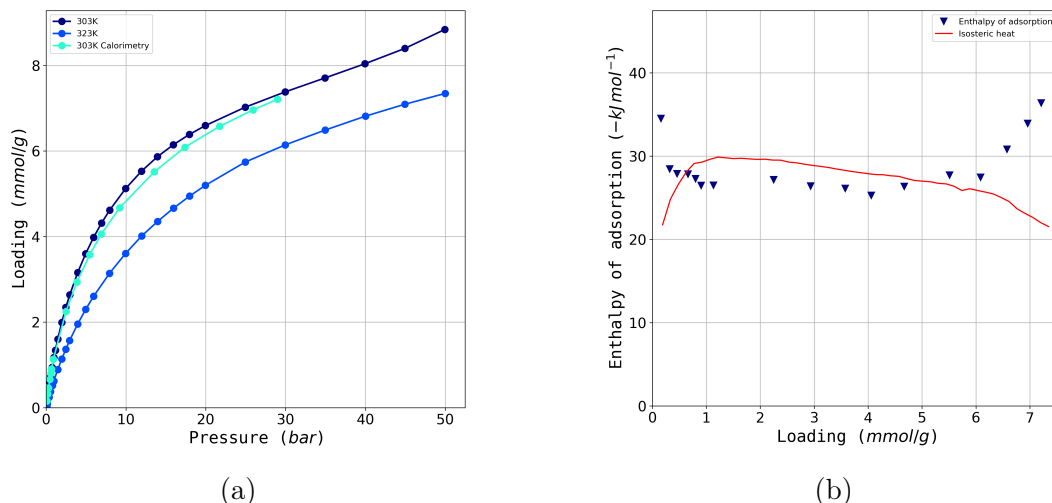


Figure 2.5.: Calculation of enthalpy of adsorption: (a) the dataset of isotherms used and (b) the calculated isosteric heat (red line) together with the measured differential enthalpy of adsorption (blue triangles)

2.4.2. Analysis of a carbon sample for gas separation applications

A sample of reference carbon Takeda 5A is to be investigated for an in-depth characterisation of the adsorption behaviour of pure gases, with a focus on describing the pore environment. Afterwards, the performance of different binary separations is evaluated, such as CO_2/N_2 and propane/propylene.

Pure gas adsorption data has been recorded at 303 K in conjunction with microcalorimetry on N_2 , CO , CO_2 , CH_4 , C_2H_6 , C_3H_6 and C_3H_8 . The complete dataset is plotted with the `pygaps.plot_iso()` function and can be seen in Figure 2.6a.

Nitrogen and carbon monoxide are similar in their adsorption behaviour, with a nearly linear isotherm and low capacities. Hydrocarbons are adsorbed with higher loadings, with both propane and propylene reaching a plateau at low pressures. Propylene is seen to have a higher capacity than propane, with packing effects as a likely cause. Carbon dioxide has the highest loading capacity of the entire dataset.

2. Extending bulk analysis of porous compounds through calorimetry

Two parameters can be useful in characterising the local pore environment before guest-guest interactions come into effect: the Henry constant at low loadings as well as the initial enthalpy of adsorption. Both can be calculated with `pyGAPS`, with several options in regard to the methodology. Here, Henry’s constant is calculated using the `pygaps.initial_henry_virial()` function, which fits a virial model to the isotherm and then takes the limit at loading approaching zero. The initial enthalpy of adsorption is obtained through the `pygaps.initial_enthalpy_comp()` function. This fits the enthalpy curve to a compound contribution from guest-host interaction, defects, guest-guest attraction and repulsion using a minimization algorithm. The results of the calculations are plotted versus the polarizability of the gas used, which can be obtained from the respective `Adsorbate` class. Figure 2.6b shows that both the parameters fall on a linear trend, which suggests that the interactions between those guests and the pore walls are mostly due to Lennard-Jones interactions. Carbon dioxide has a higher enthalpy of adsorption than the baseline due to the contribution from its quadrupole moment. There is almost a complete overlap between propane and propylene, which leads to the conclusion that the unsaturated double bond does not interact in a specific way with the carbon surface. The difference between the two isotherms is due exclusively to steric and packing effects.

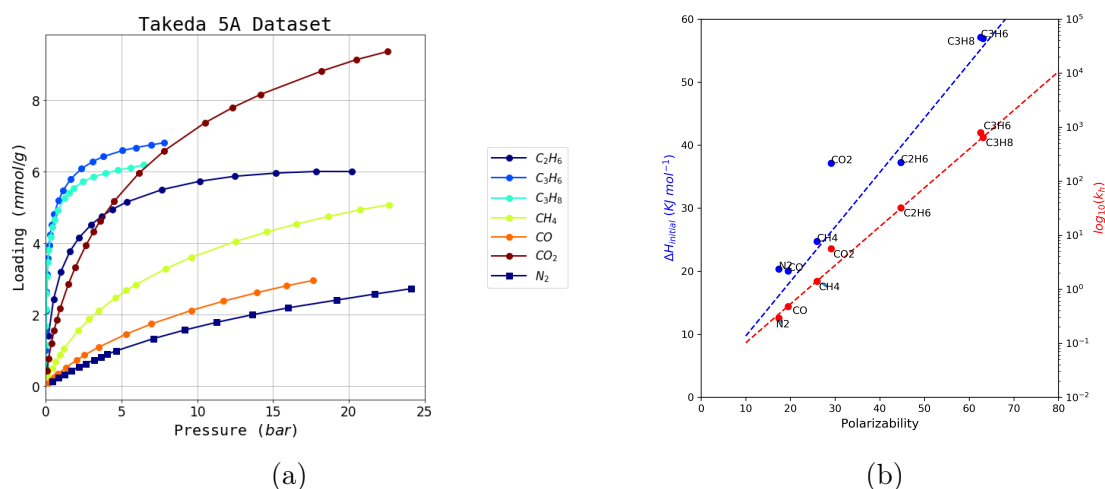


Figure 2.6.: Takeda 5A dataset processing: (a) the experimental dataset all recorded gases and (b) the calculated trends of initial heat of adsorption and Henry’s constant

2.5. Conclusion

Bibliography

- [1] Jean Rouquerol, Françoise Rouquerol, Philip L. Llewellyn, Guillaume Maurin, and Kenneth Sing. *Adsorption by Powders and Porous Solids : Principles, Methodology and Applications*. 2013. ISBN 978-0-08-097035-6.
- [2] P. L. Llewellyn, J. P. Coulomb, Y. Grillet, J. Patarin, H. Lauter, H. Reichert, and J. Rouquerol. Adsorption by MFI-type zeolites examined by isothermal microcalorimetry and neutron diffraction. 1. Argon, krypton, and methane. *Langmuir*, 9(7):1846–1851, July 1993. ISSN 0743-7463, 1520-5827. doi: 10.1021/la00031a036.
- [3] G. Maurin, P.L. Llewellyn, Th. Poyet, and B. Kuchta. Adsorption of argon and nitrogen in X-faujasites: Relationships for understanding the interactions with monovalent and divalent cations. *Microporous and Mesoporous Materials*, 79(1-3):53–59, April 2005. ISSN 13871811. doi: 10.1016/j.micromeso.2004.10.017.
- [4] Lukáš Grajciar, Andrew D. Wiersum, Philip L. Llewellyn, Jong-San Chang, and Petr Nachtigall. Understanding CO₂ Adsorption in CuBTC MOF: Comparing Combined DFT–ab Initio Calculations with Microcalorimetry Experiments. *The Journal of Physical Chemistry C*, 115(36):17925–17933, September 2011. ISSN 1932-7447. doi: 10.1021/jp206002d.
- [5] Ji Woong Yoon, You-Kyong Seo, Young Kyu Hwang, Jong-San Chang, Hervé Leclerc, Stefan Wuttke, Philippe Bazin, Alexandre Vimont, Marco Daturi, Emily Bloch, Philip L. Llewellyn, Christian Serre, Patricia Horcajada, Jean-Marc Grenèche, Alirio E. Rodrigues, and Gérard Férey. Controlled Reducibility of a Metal-Organic Framework with Coordinatively Unsaturated Sites for Preferential Gas Sorption. *Angewandte Chemie International Edition*, 49(34):5949–5952, August 2010. ISSN 14337851. doi: 10.1002/anie.201001230.
- [6] Miroslav Rubeš, Andrew D. Wiersum, Philip L. Llewellyn, Lukáš Grajciar, Ota Bludský, Petr Nachtigall, Miroslav Rubes, Andrew D. Wiersum, Philip L. Llewellyn, Lukáš Grajciar, Ota Bludský, and Petr Nachtigall. Adsorption of propane and propylene on CuBTC metal-organic framework: Combined theoretical and experimental investigation. *Journal of Physical Chemistry C*, 117(21):11159–11167, May 2013. ISSN 19327447. doi: 10.1021/jp401600v.
- [7] Jean Rouquerol, Stanislas Partyka, and Françoise Rouquerol. Calorimetric evidence for a bidimensional phase change in the monolayer of nitrogen or argon adsorbed on graphite at 77 K. *Journal of the Chemical Society, Faraday Transactions 1: Physical Chemistry in Condensed Phases*, 73:306, 1977. ISSN 0300-9599. doi: 10.1039/f19777300306.
- [8] Sandrine Bourrelly, Philip L. Llewellyn, Christian Serre, Franck Millange, Thierry Loiseau, and Gérard Férey. Different Adsorption Behaviors of Methane and Carbon Dioxide in the Isotypic Nanoporous Metal Terephthalates MIL-53 and MIL-47.

BIBLIOGRAPHY

- Journal of the American Chemical Society*, 127(39):13519–13521, October 2005. ISSN 0002-7863. doi: 10.1021/ja054668v.
- [9] Jarad A. Mason, Julia Oktawiec, Mercedes K. Taylor, Matthew R. Hudson, Julien Rodriguez, Jonathan E. Bachman, Miguel I. Gonzalez, Antonio Cervellino, Antonietta Guagliardi, Craig M. Brown, Philip L. Llewellyn, Norberto Masciocchi, and Jeffrey R. Long. Methane storage in flexible metal–organic frameworks with intrinsic thermal management. *Nature*, 527(7578):357–361, October 2015. ISSN 0028-0836, 1476-4687. doi: 10.1038/nature15732.
- [10] P. L. Llewellyn, J. P. Coulomb, Y. Grillet, J. Patarin, G. Andre, and J. Rouquerol. Adsorption by MFI-type zeolites examined by isothermal microcalorimetry and neutron diffraction. 2. Nitrogen and carbon monoxide. *Langmuir*, 9(7):1852–1856, July 1993. ISSN 0743-7463, 1520-5827. doi: 10.1021/la00031a037.
- [11] Philip L. Llewellyn and Guillaume Maurin. Gas adsorption microcalorimetry and modelling to characterise zeolites and related materials. *Comptes Rendus Chimie*, 8(3-4):283–302, March 2005. ISSN 16310748. doi: 10.1016/j.crci.2004.11.004.
- [12] E Calvet and H Prat. *Recent Progress in Microcalorimetry*. 1963. OCLC: 893676446.
- [13] Françoise Rouquerol, Jean Rouquerol, and Douglas H. Everett. Gas—solid interactions. General derivation of reaction enthalpies from the data of isothermal microcalorimetry. *Thermochimica Acta*, 41(3):311–322, November 1980. ISSN 00406031. doi: 10.1016/0040-6031(80)87207-8.

A. Common characterisation techniques

pictures?

A.1. Thermogravimetry

Thermogravimetry (TGA) is a standard laboratory technique where the weight of a sample is monitored while ambient temperature is controlled. Changes in sample mass can be correlated to physical events, such as adsorption, desorption, sample decomposition or oxidation, depending on temperature and its rate of change.

TGA experiments are carried out on approximately 15 mg of sample with a TA Instruments Q500 up to 800 °C. The sample is placed on a platinum crucible and sealed in a temperature controlled oven, under gas flow of 40 cm³ min⁻¹. Experiments can use a blanket of either air or argon. The temperature ramp can be specified directly and should be chosen to ensure that the sample is in equilibrium with the oven temperature and no thermal conductivity effects come into play. Alternatively, a dynamic “Hi-Res” mode can be used which allows for automatic cessation of heating rate while the sample undergoes mass loss.

The main purpose of thermogravimetry as used in this thesis is the determination of sample decomposition temperature, to ensure that thermal activation prior to adsorption is complete and that all guest molecules have been removed without loss of structure. To this end, experiments are performed under an inert atmosphere (argon), and the sample activation temperature is chosen as 50 °C to 100 °C lower than the sample decomposition temperature.

A.2. Bulk density determination

Bulk density is a useful metric for the industrial use of adsorbent materials, as their volume plays a critical role in equipment sizing.

Bulk density is determined by weighing 1.5 ml empty glass vessels and settling the MOFs inside. Powder materials are then added in small increments and settled through vibration between each addition. The full vessel is finally weighed, which allowed the bulk density to be determined. The same cell is used in all experiments, with cleaning through sonication between each experiment.

A.3. Skeletal density determination

True density or skeletal density is determined through gas pycnometry in a MicrotracBEL BELSORP-max apparatus. Helium is chosen as the fluid of choice as it is assumed to be non-adsorbing.

The volume of a glass sample cell (V_c) is precisely measured through dosing of the reference volume with helium up to (p_1), then opening the valve connecting the two and allowing the gas to expand up to (p_2). Afterwards approximately 50 mg of sample are weighed and inserted in a glass sample cell. After sample activation using the supplied electric heater to ensure no solvent residue is left in the pores, the same procedure is repeated to determine the volume of the cell and the adsorbent. With the volume of the sample determined, the density can be calculated by.

$$V_s = V_c + \frac{V_r}{1 - \frac{p_1}{p_2}} \quad (\text{A.1})$$

A.4. Nitrogen physisorption at 77 K

Nitrogen adsorption experiments are carried out on a Micromeritics Triflex apparatus. Approximately 60 mg of sample are used for each measurement. Empty glass cells are weighed and filled with the samples, which are then activated in a Micromeritics Smart VacPrep up to their respective activation temperature under vacuum and then back-filled with an inert atmosphere. After sample activation, the cells are re-weighed to determine the precise sample mass. The cells are covered with a porous mantle which allows for a constant temperature gradient during measurement by wicking liquid nitrogen around the cell. Finally, the cells are immersed in a liquid nitrogen bath and the adsorption isotherm is recorded using the volumetric method. A separate cell is used to condense the adsorptive throughout the measurement for accurate determination of its saturation pressure.

A.5. Vapour physisorption at 298 K

Vapour adsorption isotherms throughout this work are measured using a MicrotracBEL BELSORP-max apparatus in vapour mode. Glass cells are first weighed and then filled with about 50 mg of sample. The vials are then heated under vacuum up to the activation temperature of the material and re-weighed in order to measure the exact sample mass without adsorbed guests. The cells are then immersed in a mineral oil bath kept at 298 K. To ensure that the cold point of the system occurs in the material and to prevent condensation on cell walls, the reference volume, dead space and vapour source are temperature controlled through an insulated enclosure.

A.6. Gravimetric isotherms

The gravimetric isotherms in this thesis are obtained using a commercial Rubotherm GmbH balance. Approximately 1 g of dried sample is used for these experiments. Samples are activated in situ by heating under vacuum. The gas is introduced using a step-by-step method, and equilibrium is assumed to have been reached when the variation of weight remained below 30 μg over a 15 min interval. The volume of the sample is determined from a blank experiment with helium as the non-adsorbing gas and used in combination with the gas density measured by the Rubotherm balance to compensate for buoyancy.

A.7. High throughput isotherm measurement

A high-throughput gas adsorption apparatus is presented for the evaluation of adsorbents of interest in gas storage and separation applications. This instrument is capable of measuring complete adsorption isotherms up to 50 bar on six samples in parallel using as little as 60 mg of material. Multiple adsorption cycles can be carried out and four gases can be used sequentially, giving as many as 24 adsorption isotherms in 24 h.⁽¹⁾

A.8. Powder X-ray diffraction

A.9. Nuclear magnetic resonance

Bibliography

- [1] Andrew D. Wiersum, Christophe Giovannangeli, Dominique Vincent, Emily Bloch, Helge Reinsch, Norbert Stock, Ji Sun Lee, Jong-San Chang, and Philip L. Llewellyn. Experimental Screening of Porous Materials for High Pressure Gas Adsorption and Evaluation in Gas Separations: Application to MOFs (MIL-100 and CAU-10). *ACS Combinatorial Science*, 15(2):111–119, February 2013. ISSN 2156-8952. doi: 10.1021/co300128w.

B. Synthesis method of referenced materials

B.1. Takeda 5A reference carbon

The Takeda 5A carbon was purchased directly from the Takeda corporation. The sample was activated at 250 °C under secondary vacuum (5 mbar) before any measurements.

full
char-
acteri-
zation

B.2. MCM-41 controlled pore glass

MCM-41 (Mobil Composition of Matter No. 41) is a mesoporous silica (SiO_2) material with a narrow pore distribution. First synthesised by the Mobil Oil Corporation, it is produced through templated synthesis using mycelle-forming surfactants. The material referenced in this thesis was purchased from Sigma-Aldrich. The activation procedure consists of heating at 250 °C under secondary vacuum (5 mbar).

B.3. Zr fumarate MOF

The synthesis of the Zr fumarate was performed in Peter Behren's group in Hannover, through modulated synthesis. This MOF can only be synthesised through the addition of a modulator, in this case fumaric acid, to the ongoing reactor, as detailed in the original publication.⁽¹⁾

The procedure goes as follows: ZrCl_4 (0.517 mmol, 1 eq) and fumaric acid (1.550 mmol, 3 eq) are dissolved in 20 mL N,N-dimethylformamide (DMF) and placed in a 100 mL glass flask at room temperature. 20 equivalents of formic acid were added. The glass flasks were Teflon-capped and heated in an oven at 120 °C for 24 h. After cooling, the white precipitate was washed with 10 mL DMF and 10 mL ethanol, respectively. The washing process was carried out by centrifugation and redispersion of the white powder, which was then dried at room temperature over night

B.4. UiO-66(Zr) for defect study

The UiO-66(Zr) sample preparation was adapted from Shearer et al.⁽²⁾ as follows: ZrCl_4 (1.55 g, 6.65 mmol), an excess of terephthalic acid (BDC) (1.68 g, 10.11 mmol), HCl 37 % solution (0.2 mL, 3.25 mmol) and N,N'-dimethylformamide (DMF) (200 mL,

2.58 mol) were added to a 250 mL pressure resistant Schott bottle. The mixture was stirred for 10 min, followed by incubation in a convection oven at 130 °C for 24 h. The resulting white precipitate was washed with fresh DMF (3× 50 mL) followed by ethanol (3× 50 mL) over the course of 48 h and dried at 60 °C. After drying, the sample was activated on a vacuum oven by heating at 200 °C under vacuum for 12 h. The yield was 78 % white microcrystalline powder. Before the experiment, the sample was calcined at 200 °C under vacuum (5 mbar) to remove any residual solvents from the framework.

B.5. UiO-66(Zr) for shaping study

The scaled-up synthesis of UiO-66(Zr) was carried out in a 5 L glass reactor (Reactor Master, Syrris, equipped with a reflux condenser and a Teflon-lined mechanical stirrer) according to a previously reported method.⁽³⁾ In short, 462 g (2.8 mol) of H₂BDC (98%) was initially dissolved in 2.5 L of dimethyl formamide (DMF, 2.36 kg, 32.3 mol) at room temperature. Then, 896 g (2.8 mol) of ZrOCl₂ · 8H₂O (98%) and 465 mL of 37% HCl (548 g, 15 mol) were added to the mixture. The molar ratio of the final ZrOCl₂ · 8H₂O/H₂BDC/DMF/HCl mixture was 1 : 1 : 11.6 : 5.4. The reaction mixture was vigorously stirred to obtain a homogeneous gel. The mixture was then heated to 423 K at a rate of 1 K min⁻¹ and maintained at this temperature for 6 h in the reactor without stirring, leading to a crystalline UiO-66(Zr) solid. The resulting product (510 g) was recovered from the slurry by filtration, redispersed in 7 L of DMF at 333 K for 6 h under stirring, and recovered by filtration. The same procedure was repeated twice, using methanol (MeOH) instead of DMF. The solid product was finally dried at 373 K overnight.

B.6. MIL-100(Fe) for shaping study

The synthesis of the MOF for the shaping study was done at the KRICT institute using a previously published method.⁽⁴⁾ To synthesise the MIL-100(Fe) material Fe(NO₃)₃ was completely dissolved in water. Then, trimesic acid (BTC) was added to the solution; the resulting mixture was stirred at room temperature for 1 h. The final composition was Fe(NO₃)₃ · 9 H₂O:0.67 BTC:*n* H₂O (*x*= 55–280). The reactant mixture was heated at 433 K for 12 h using a Teflon-lined pressure vessel. The synthesized solid was filtered and washed with deionized (DI) water. Further washing was carried out with DI water and ethanol at 343 K for 3 h and purified with a 38 mM NH₄F solution at 343 K for 3 h. The solid was finally dried overnight at less than 373 K in air.

B.7. MIL-127(Fe) for shaping study

MIL-127(Fe) was synthesized by reaction of Fe(ClO₄)₃ · 6 H₂O (3.27 g, 9.2 mmol) and C₁₆N₂O₈H₆ (3.3 g) in DMF (415 mL) and hydrofluoric acid (5 M, 2.7 mL) at 423 K in a Teflon flask. The obtained orange crystals were placed in DMF (100 mL) and

stirred at ambient temperature for 5 h. The final product was kept at 375 K overnight. MIL-127(Fe) was synthesized by reaction of $\text{Fe}(\text{ClO}_4)_3 \cdot 6 \text{H}_2\text{O}$ (3.27 g, 9.2 mmol) and $\text{C}_{16}\text{N}_2\text{O}_8\text{H}_6$ (3.3 g) in DMF (415 mL) and hydrofluoric acid (5 M, 2.7 mL) at 423 K in a Teflon flask. The obtained orange crystals were placed in DMF (100 mL) and stirred at ambient temperature for 5 h. The final product was kept at 375 K overnight.

Bibliography

- [1] Gesa Wißmann, Andreas Schaate, Sebastian Lilienthal, Imke Bremer, Andreas M. Schneider, and Peter Behrens. Modulated synthesis of Zr-fumarate MOF. *Microporous and Mesoporous Materials*, 152:64–70, April 2012. ISSN 13871811. doi: 10.1016/j.micromeso.2011.12.010.
- [2] Greig C. Shearer, Sachin Chavan, Jayashree Ethiraj, Jenny G. Vitillo, Stian Svelle, Unni Olsbye, Carlo Lamberti, Silvia Bordiga, and Karl Petter Lillerud. Tuned to Perfection: Ironing Out the Defects in Metal–Organic Framework UiO-66. *Chemistry of Materials*, 26(14):4068–4071, July 2014. ISSN 0897-4756, 1520-5002. doi: 10.1021/cm501859p.
- [3] Florence Ragon, Patricia Horcajada, Hubert Chevreau, Young Kyu Hwang, U-Hwang Lee, Stuart R. Miller, Thomas Devic, Jong-San Chang, and Christian Serre. In Situ Energy-Dispersive X-ray Diffraction for the Synthesis Optimization and Scale-up of the Porous Zirconium Terephthalate UiO-66. *Inorganic Chemistry*, 53(5):2491–2500, March 2014. ISSN 0020-1669, 1520-510X. doi: 10.1021/ic402514n.
- [4] Felix Jeremias, Stefan K. Henninger, and Christoph Janiak. Ambient pressure synthesis of MIL-100(Fe) MOF from homogeneous solution using a redox pathway. *Dalton Transactions*, 45(20):8637–8644, 2016. ISSN 1477-9226, 1477-9234. doi: 10.1039/C6DT01179A.